# The Old Dalby landslide: rock physics and electrical resistivity tomography monitoring

**Auteur :** Guérin, Alexis
**Promoteur(s) :** Nguyen, Frederic
**Faculté :** Faculté des Sciences appliquées
**Diplôme :** Master en ingénieur civil des mines et géologue, à finalité spécialisée en géologie de l'ingénieur et de l'environnement
**Année académique :** 2017-2018
**URI/URL :** http://hdl.handle.net/2268.2/4635

# The Old Dalby landslide: rock physics and electrical resistivity tomography monitoring

Alexis Guérin
supervised by Dr. Frédéric Nguyen
Master in Mining and Geological Engineering
Academic year 2017-2018

## Representative illustrations

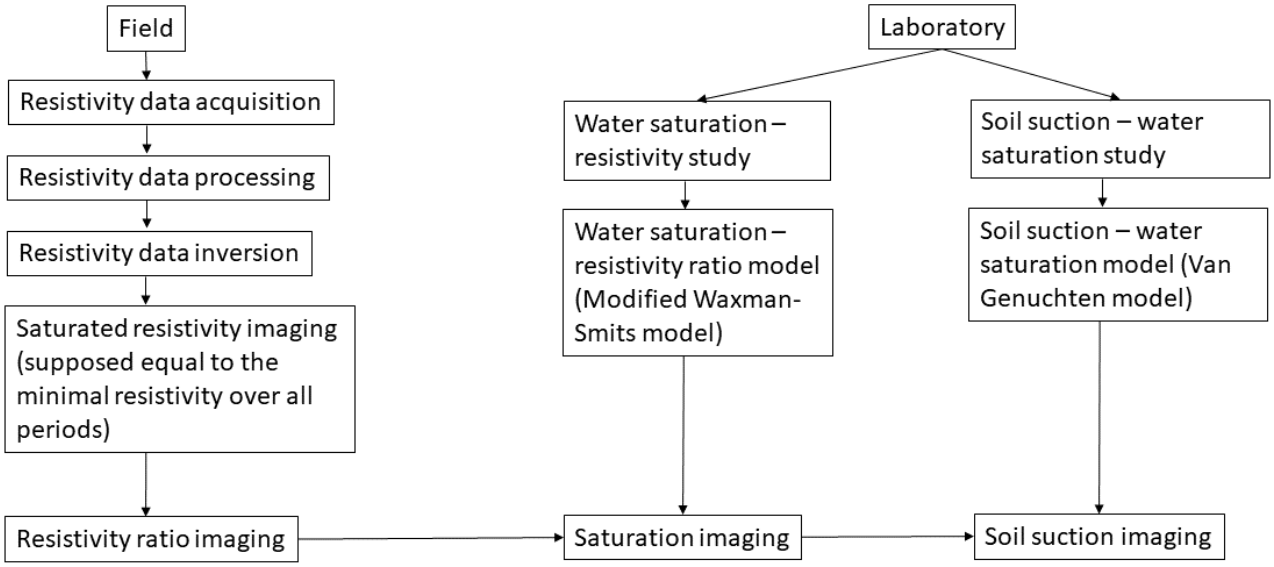


Figure 1: Overview of the data processing from the laboratory and field data acquisition to the saturation and soil suction imaging

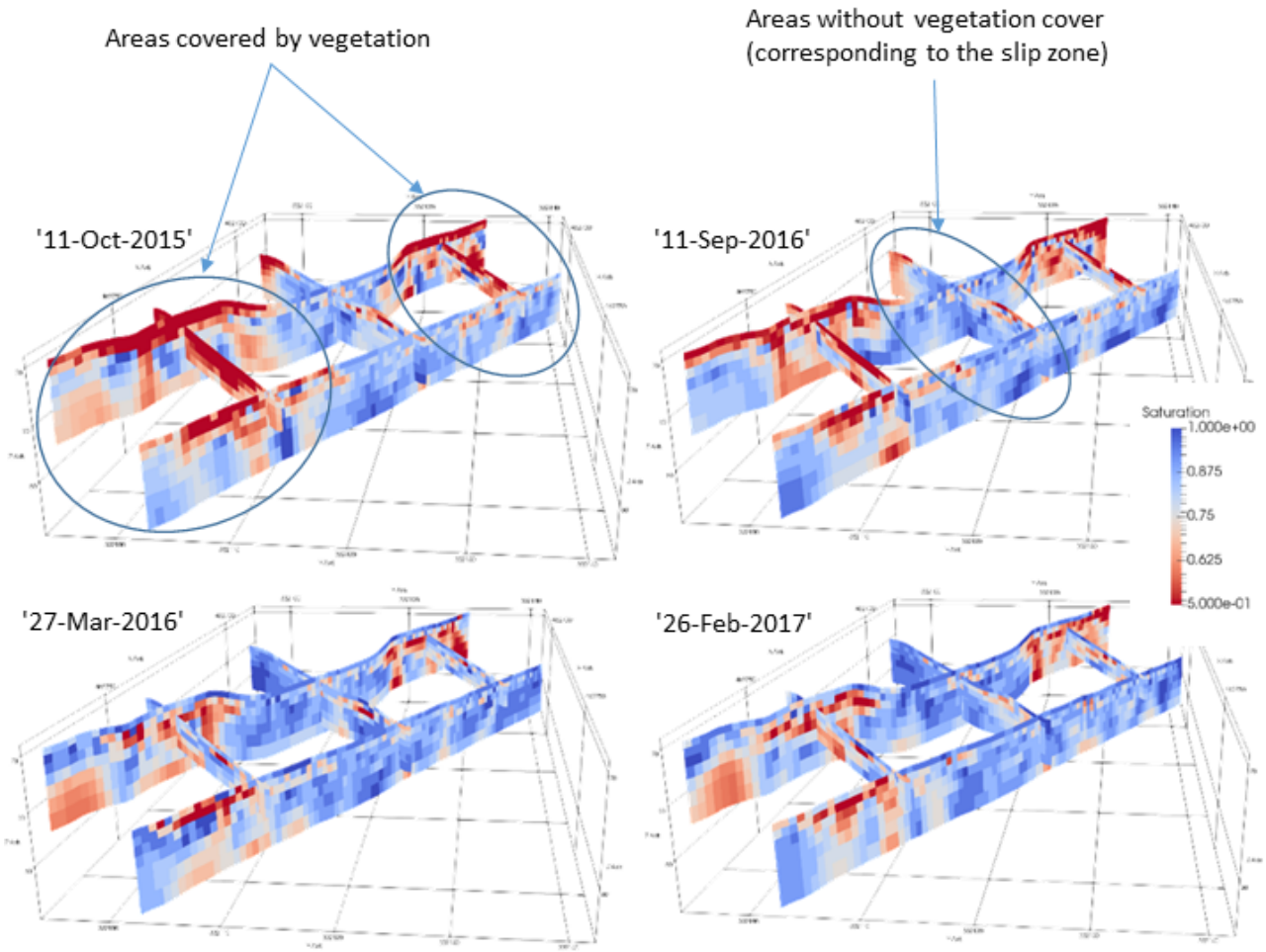


Figure 2: ERT-derived saturation imaging of the Old Dalby relict landslide

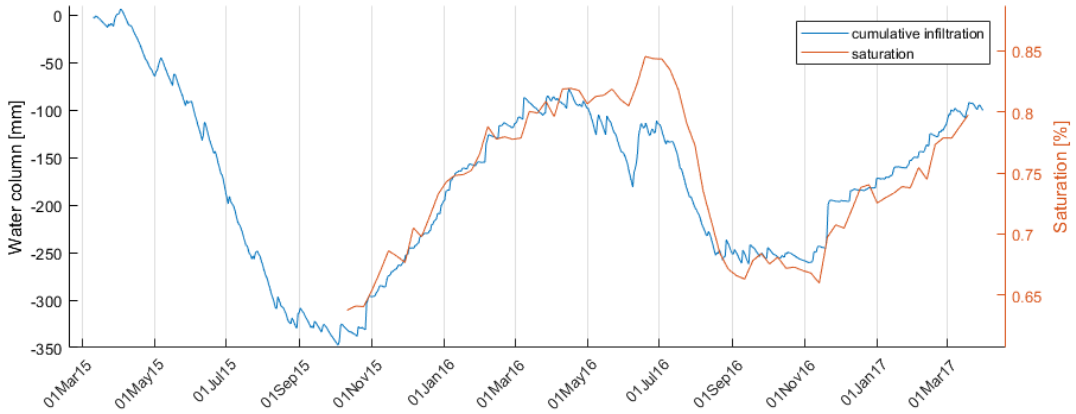


Figure 3: Comparison between the cumulative infiltration measured at the weather station and the imaged saturation in the top 3 meters of Line 2

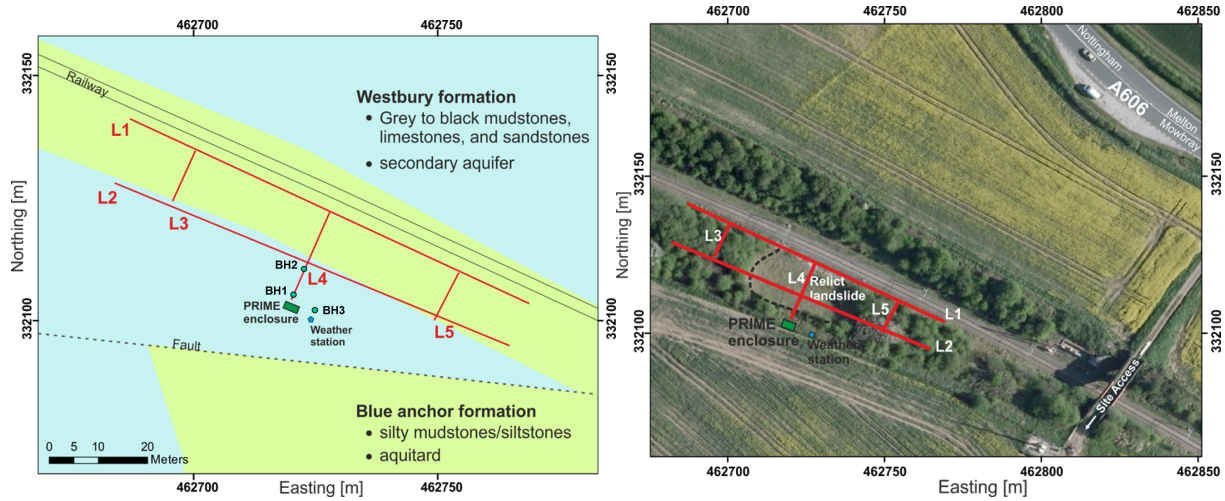


Figure 4: Location and geology of Old Dalby

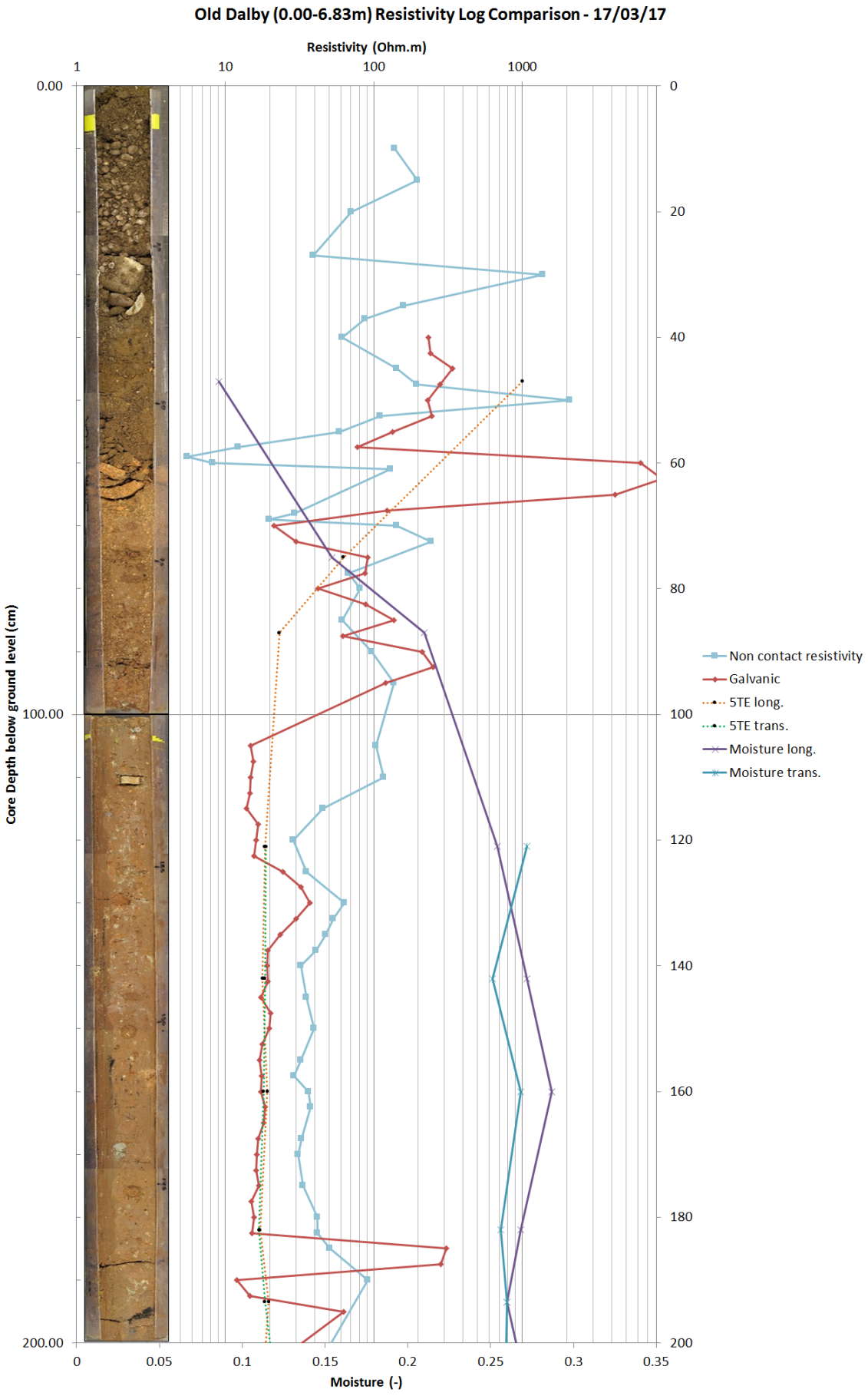
Old Dalby (0.00-6.83m) Resistivity Log Comparison - 17/03/17
Resistivity (Ohm.m)
1
10
100
1000
0.00
100.00
200.00
Core Depth below ground level (cm)
0
20
40
60
80
100
120
140
160
180
200
0
0.05
0.1
0.15
0.2
0.25
0.3
0.35
Moisture (-)
Non contact resistivity
Galvanic
5TE long.
5TE trans.
Moisture long.
Moisture trans.

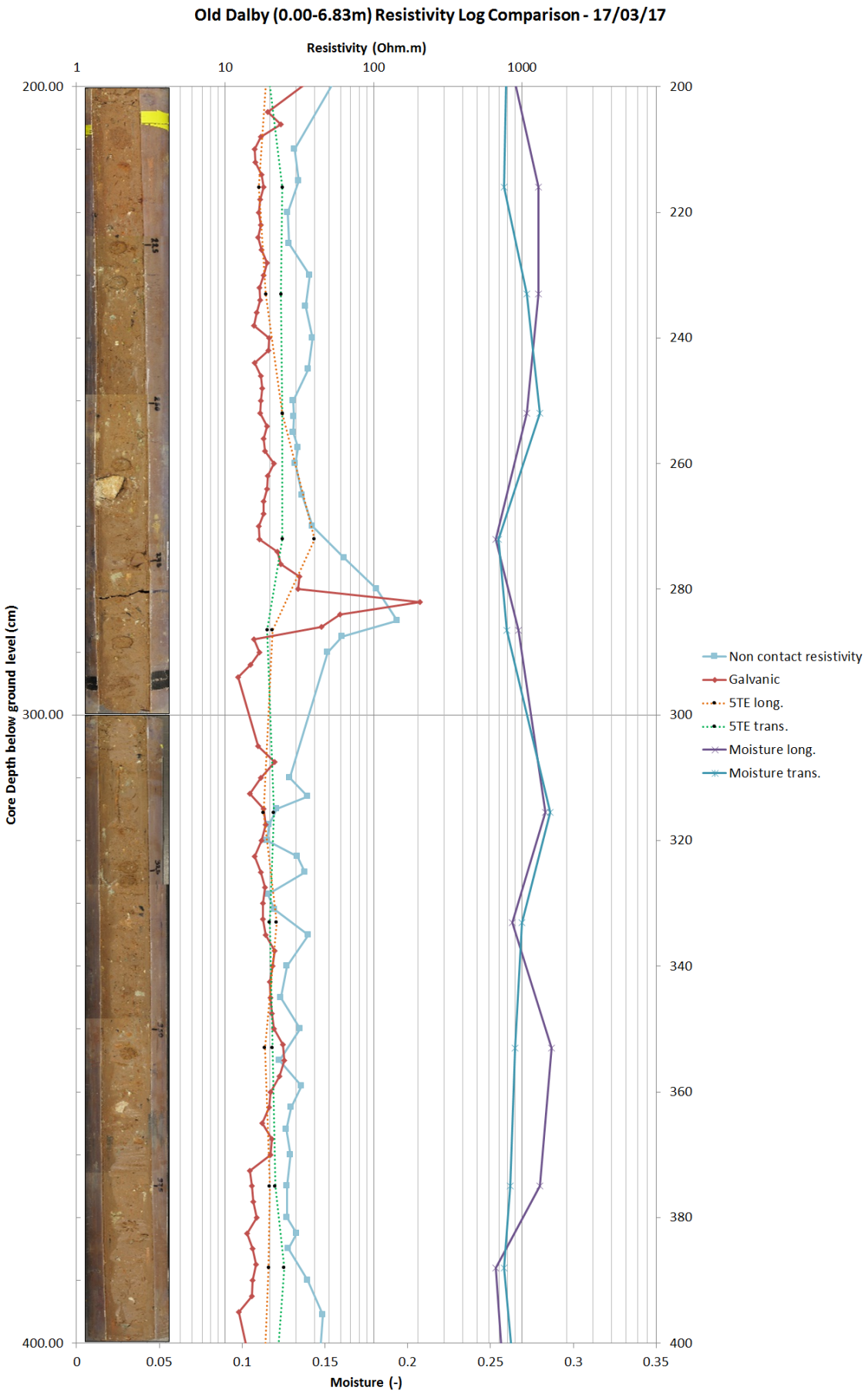
Old Dalby (0.00-6.83m) Resistivity Log Comparison - 17/03/17
Resistivity (Ohm.m)
1
10
100
1000
200.00
300.00
400.00
Core Depth below ground level (cm)
200
220
240
260
280
300
320
340
360
380
400
0
0.05
0.1
0.15
0.2
0.25
0.3
0.35
Moisture (-)
Non contact resistivity
Galvanic
5TE long.
5TE trans.
Moisture long.
Moisture trans.

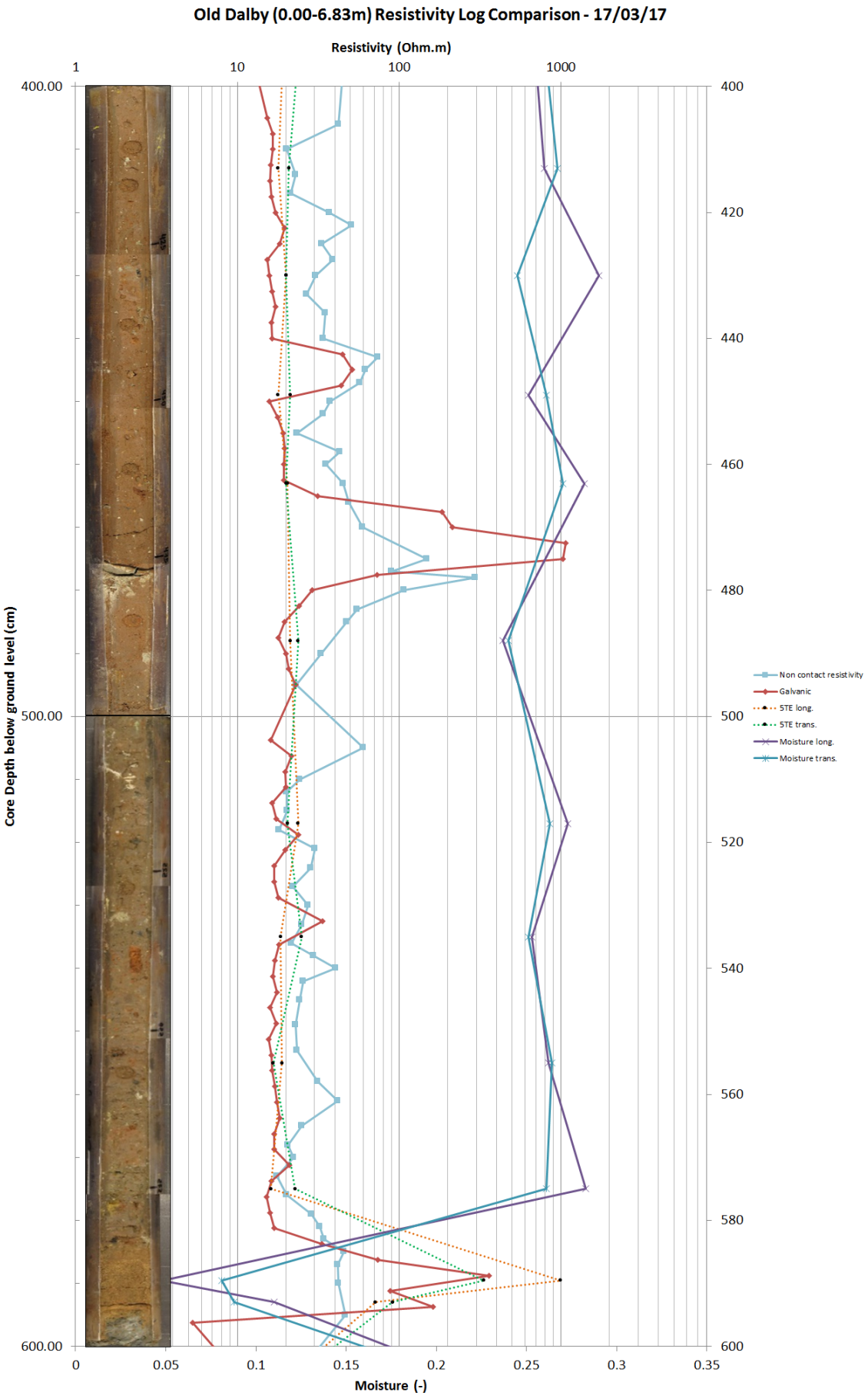
Old Dalby (0.00-6.83m) Resistivity Log Comparison - 17/03/17
Resistivity (Ohm.m)
1
10
100
1000
400.00
500.00
600.00
Core Depth below ground level (cm)
400
420
440
460
480
500
520
540
560
580
600
0
0.05
0.1
0.15
0.2
0.25
0.3
0.35
Moisture (-)
Non contact resistivity
Galvanic
5TE long.
5TE trans.
Moisture long.
Moisture trans.

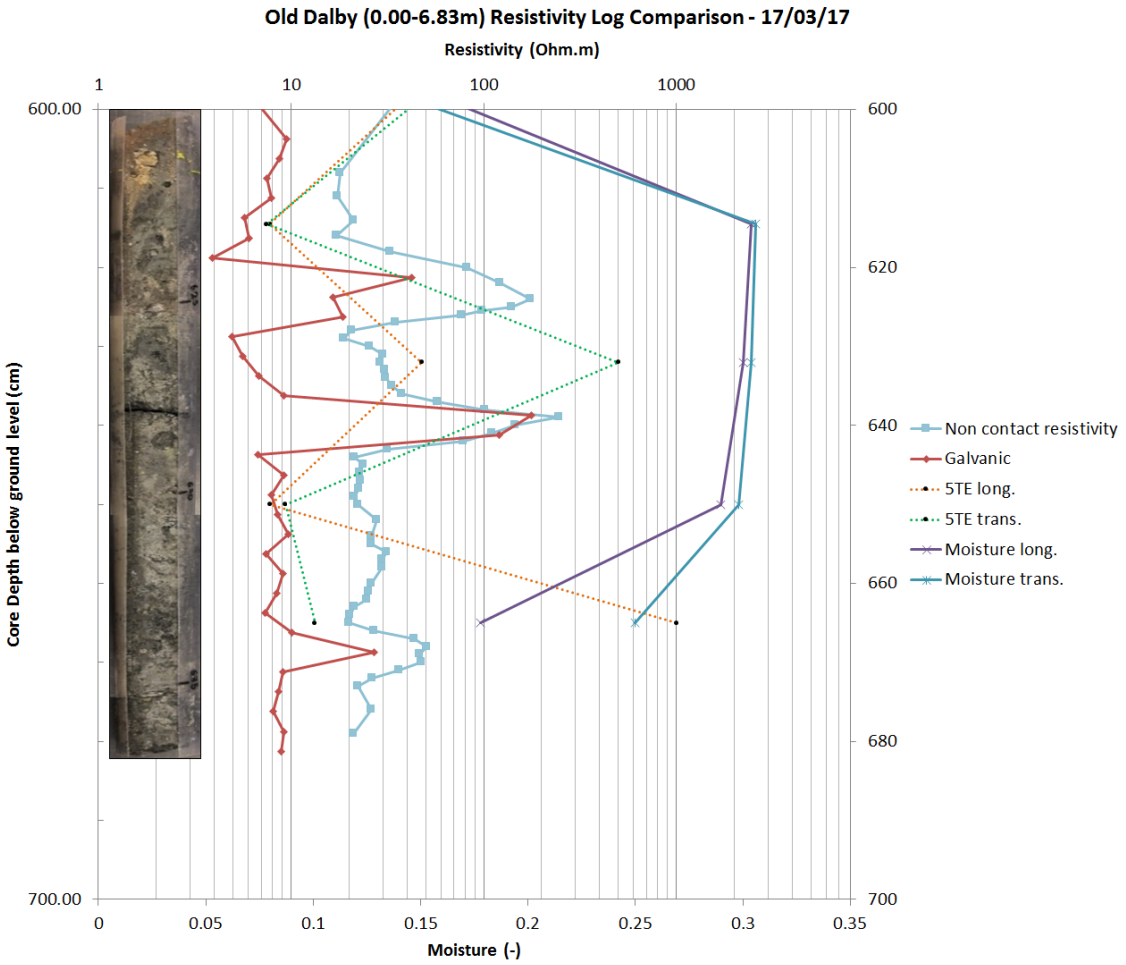


Figure 5: Old Dalby core. Comparison of the non contact resistivity imaging, with the galvanic resistivity measurements and the 5TE resistivity and moisture measurements

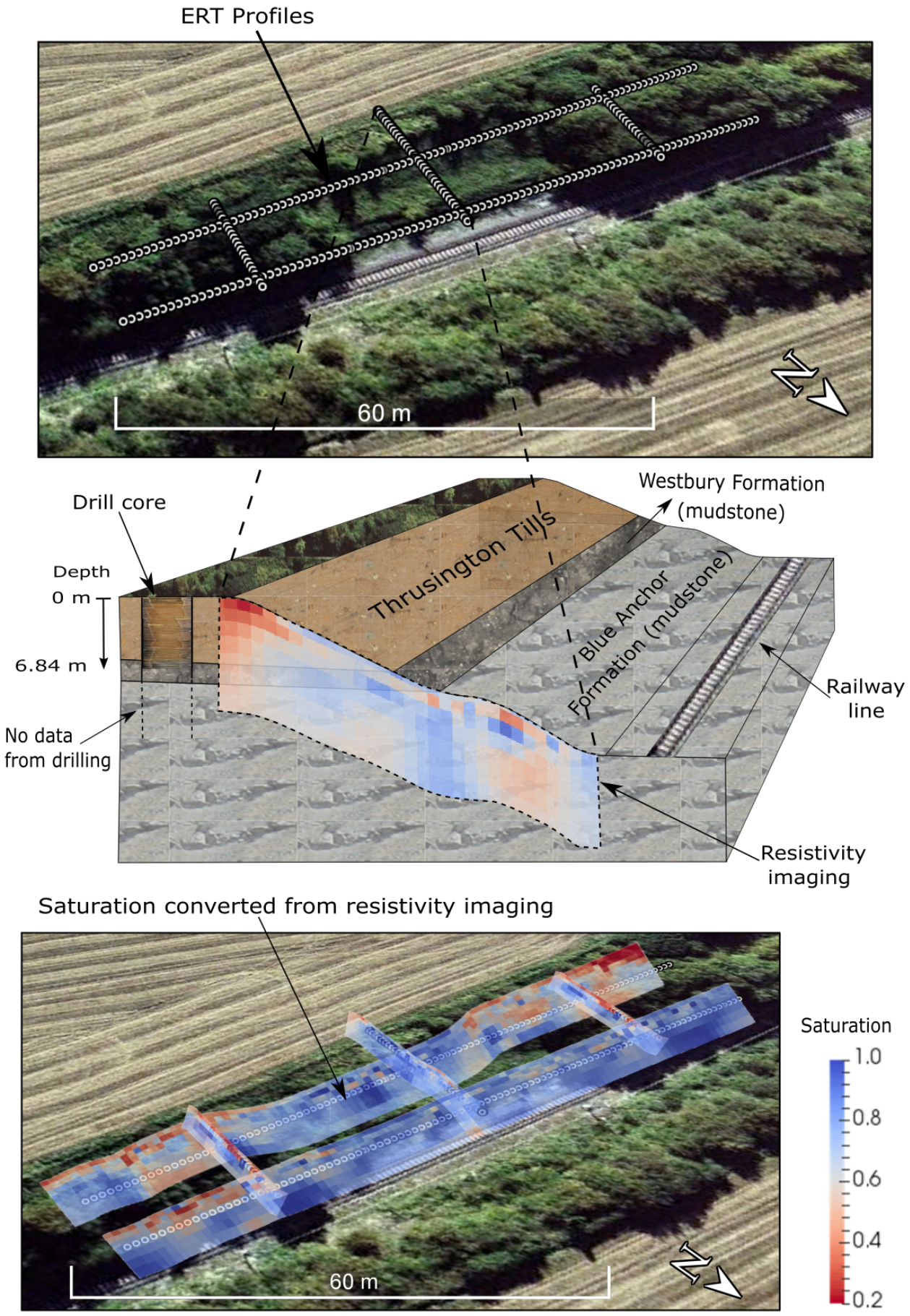


Figure 6: Old Dalby landslide geological context

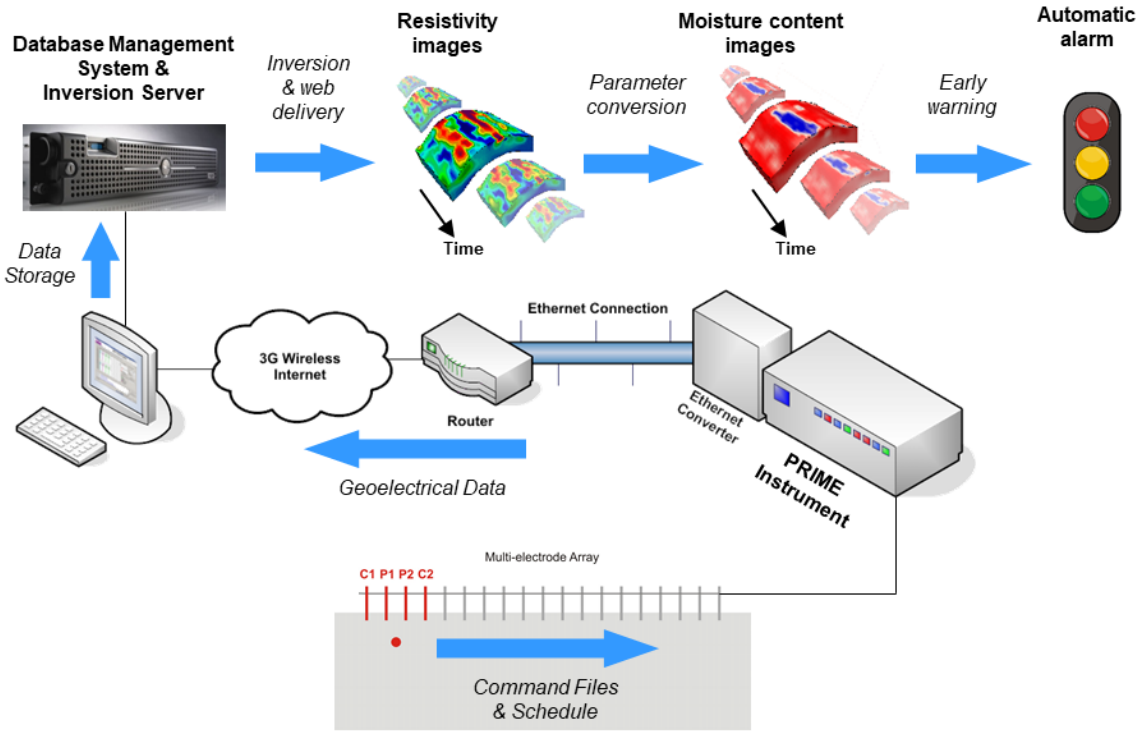


Figure 7: Prime system principle

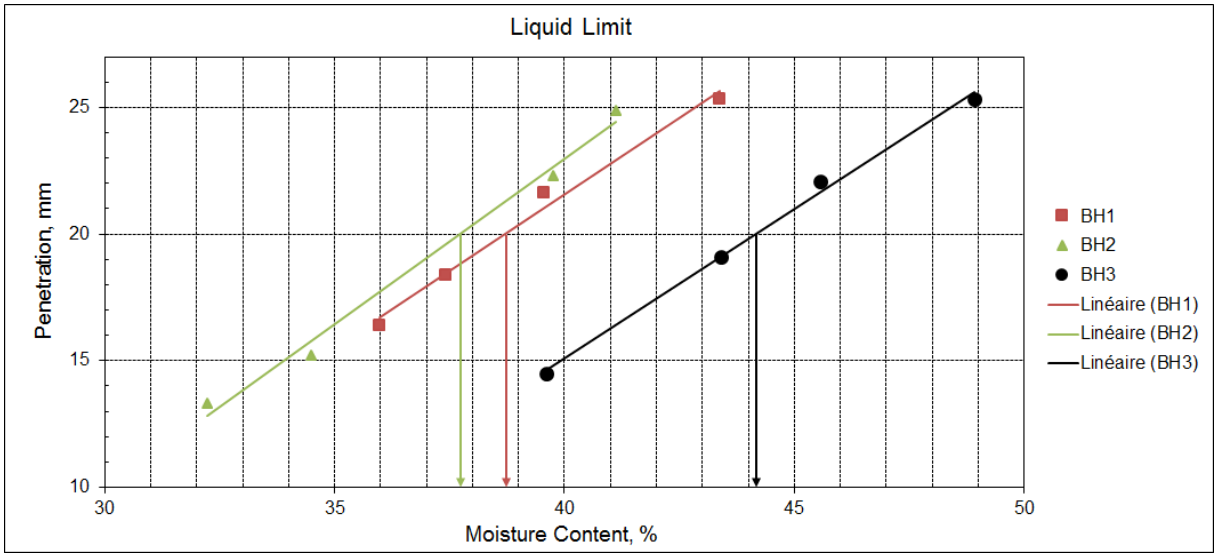


Figure 8: Liquid limit

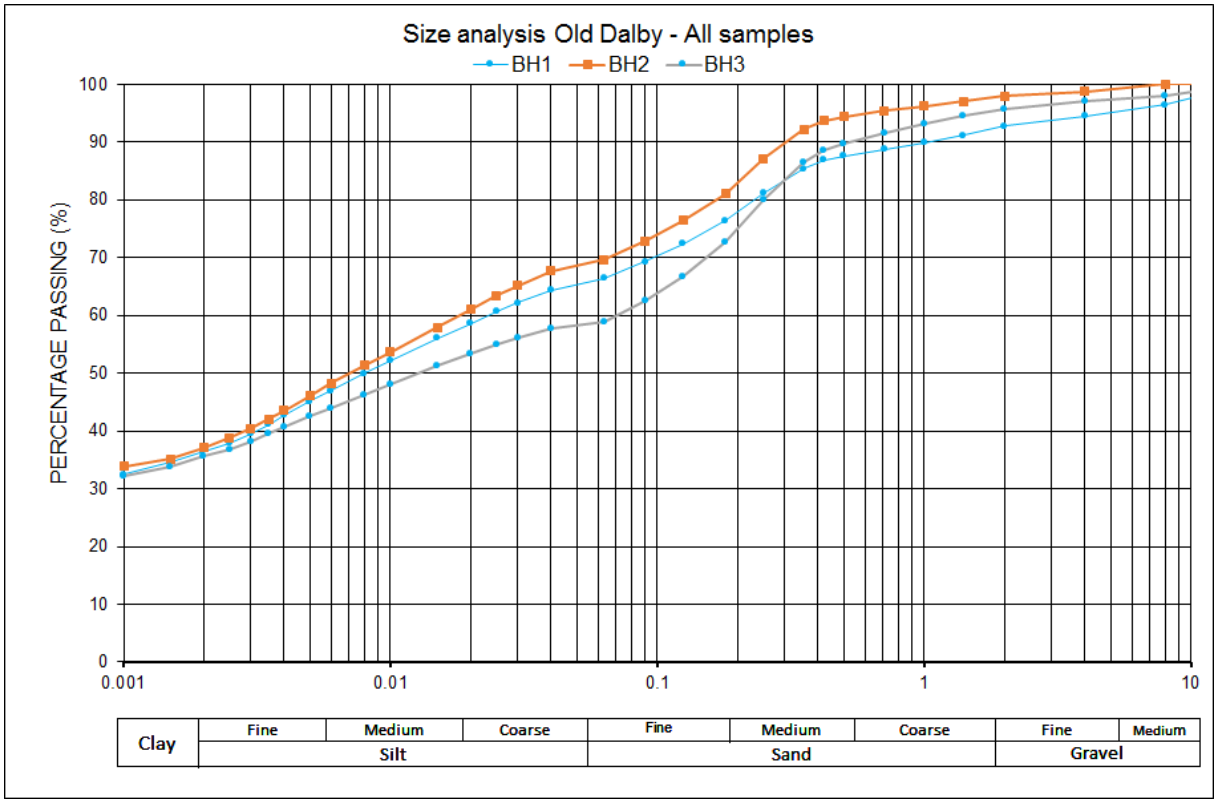


Figure 9: Old Dalby Particle Size Analysis

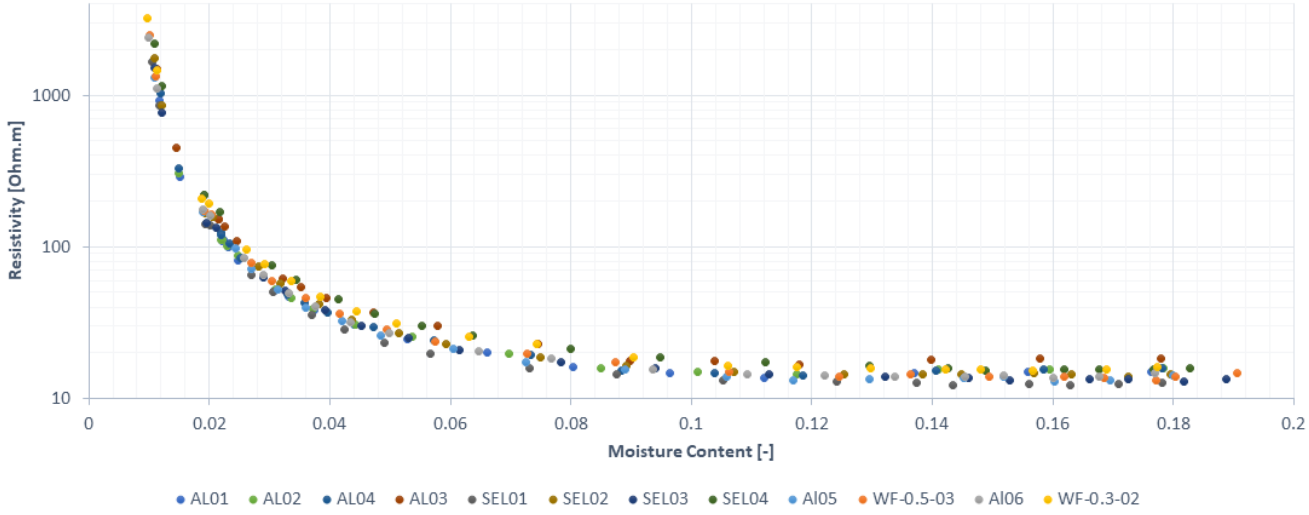


Figure 10: Resistivity-Moisture dataset from the laboratory characterization of re-compacted samples from Old Dalby

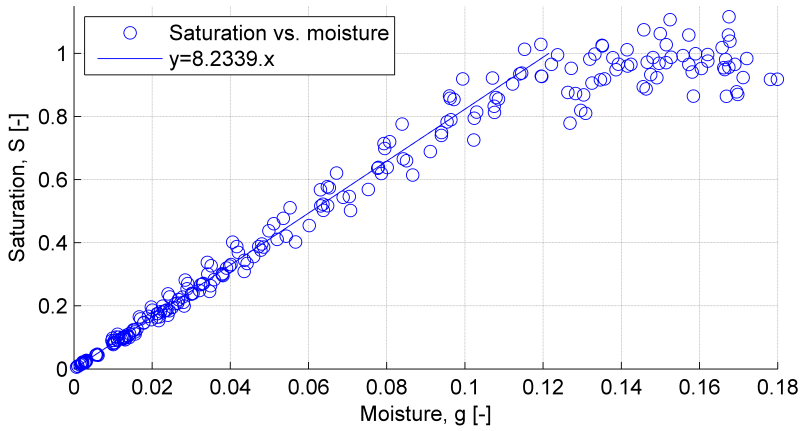


Figure 11: Moisture-saturation scatterplot.

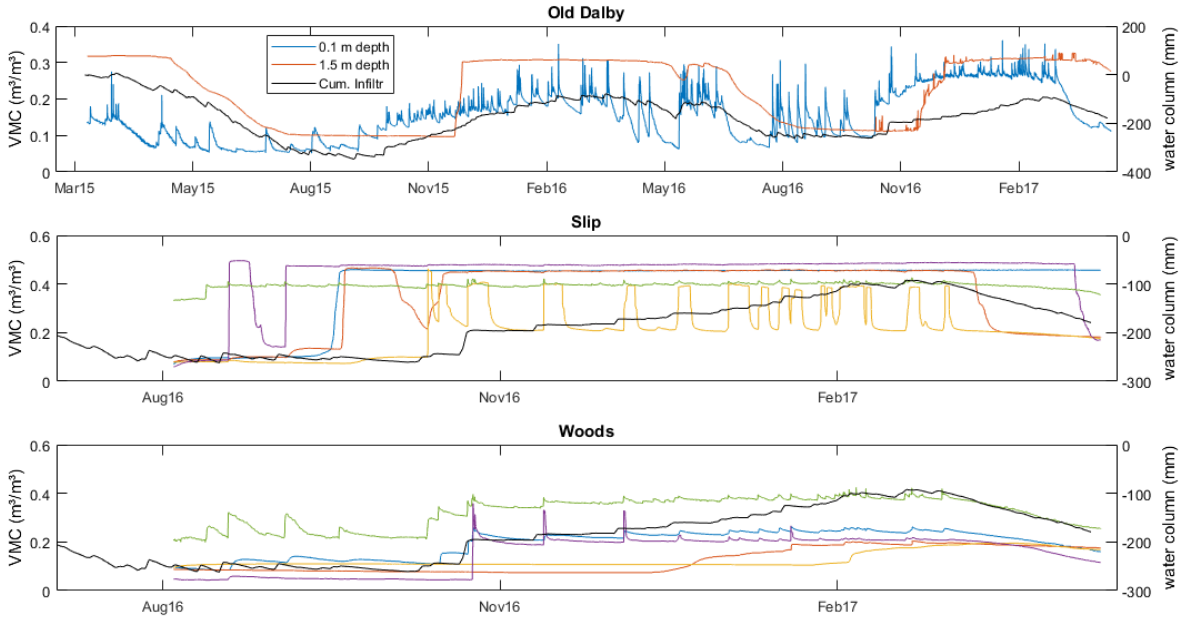


Figure 12: Comparison between cumulative infiltration data and in-situ 5TE moisture sensors

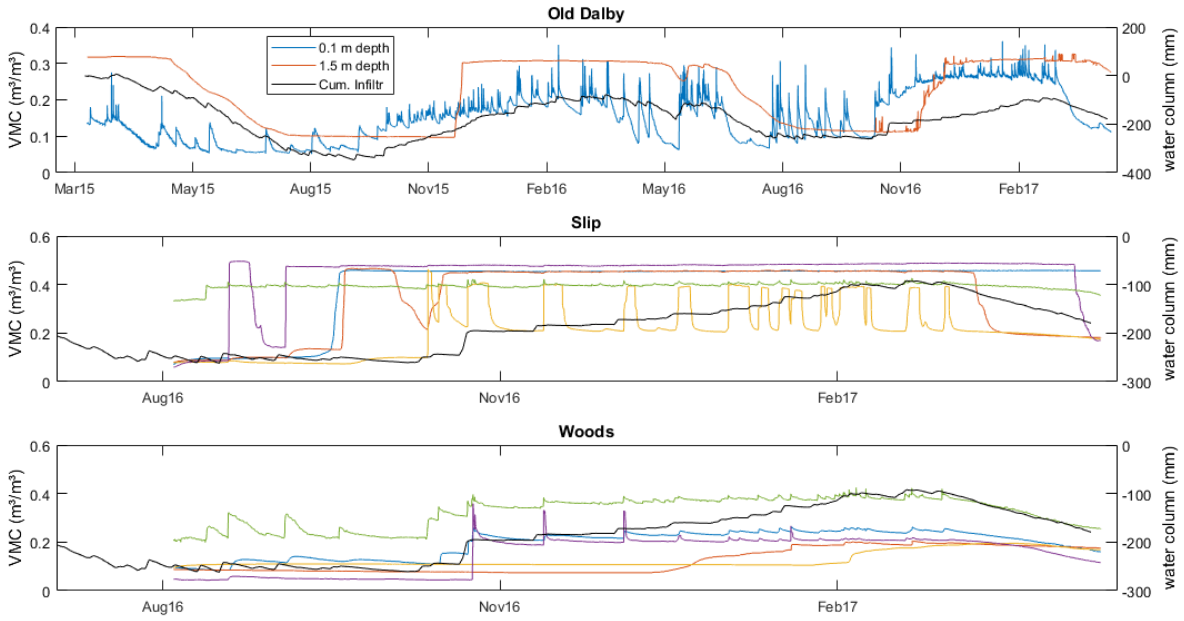


Figure 13: Comparison between cumulative infiltration data and in-situ 5TE moisture sensors

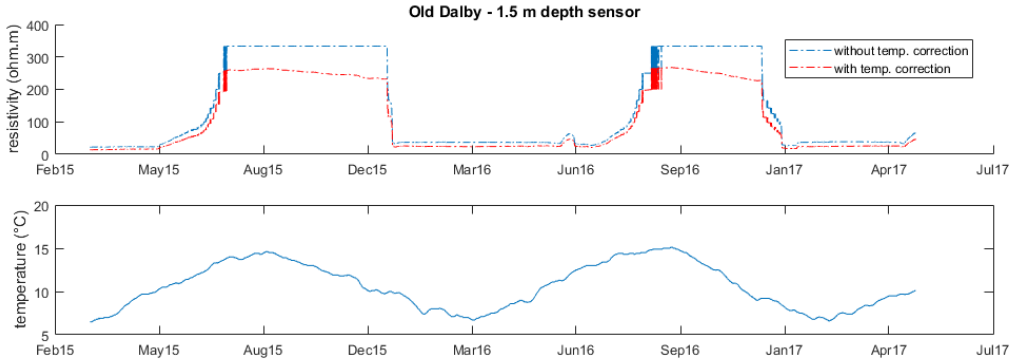


Figure 14: Effect of temperature correction on resistivity data

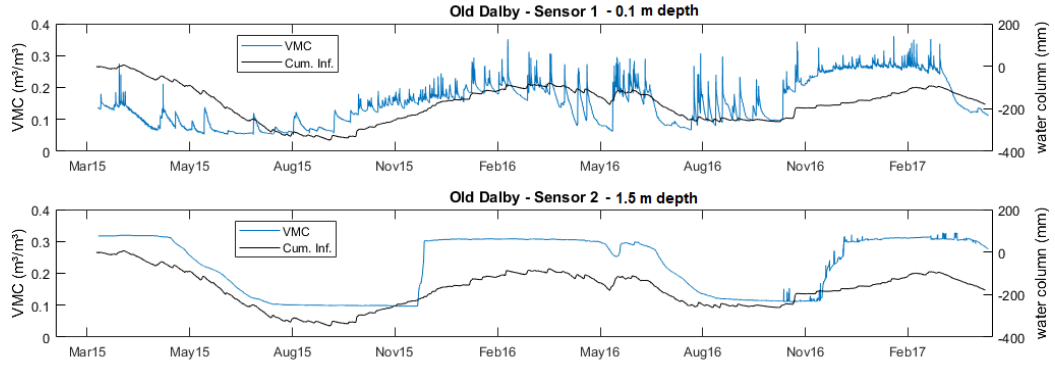


Figure 15: Comparison between the 5TE moisture content measurements and the effective infiltration calculated from the weather monitoring

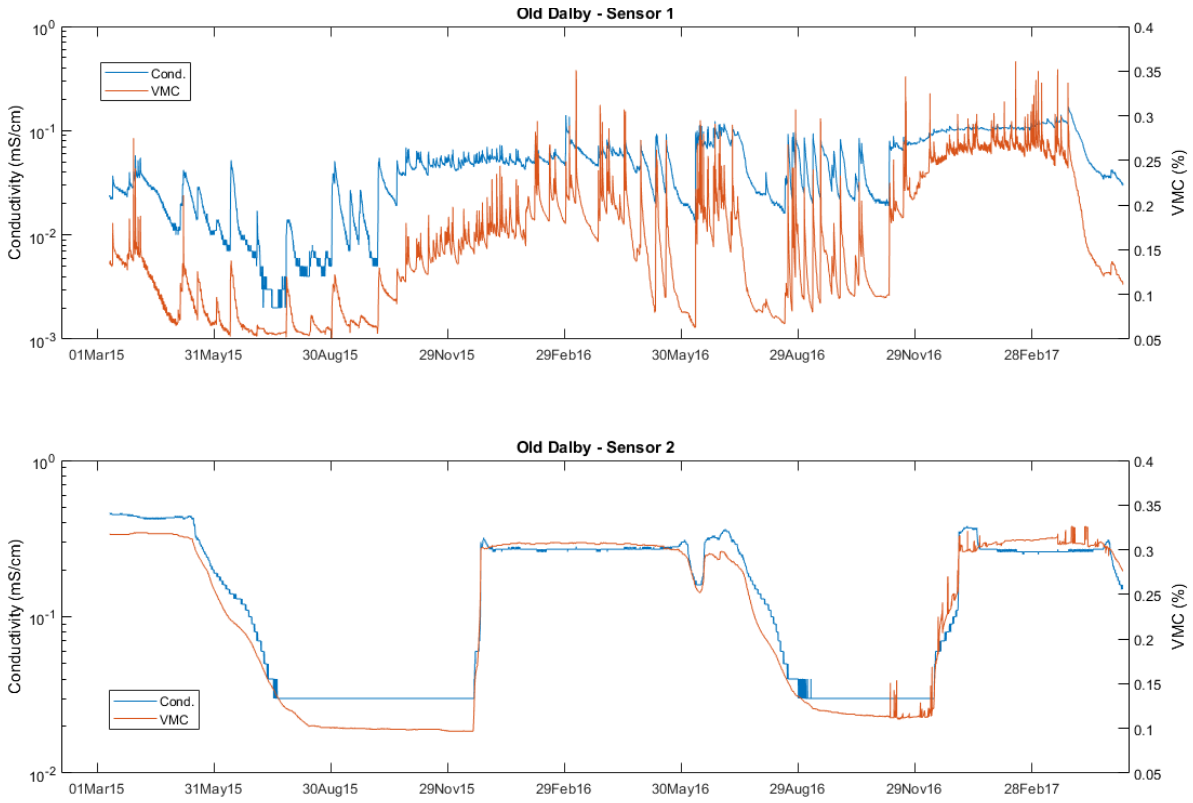


Figure 16: Comparison between the conductivity and the moisture measurement of the 5TE. Moisture and conductivity are evaluated with independent measurement methods.

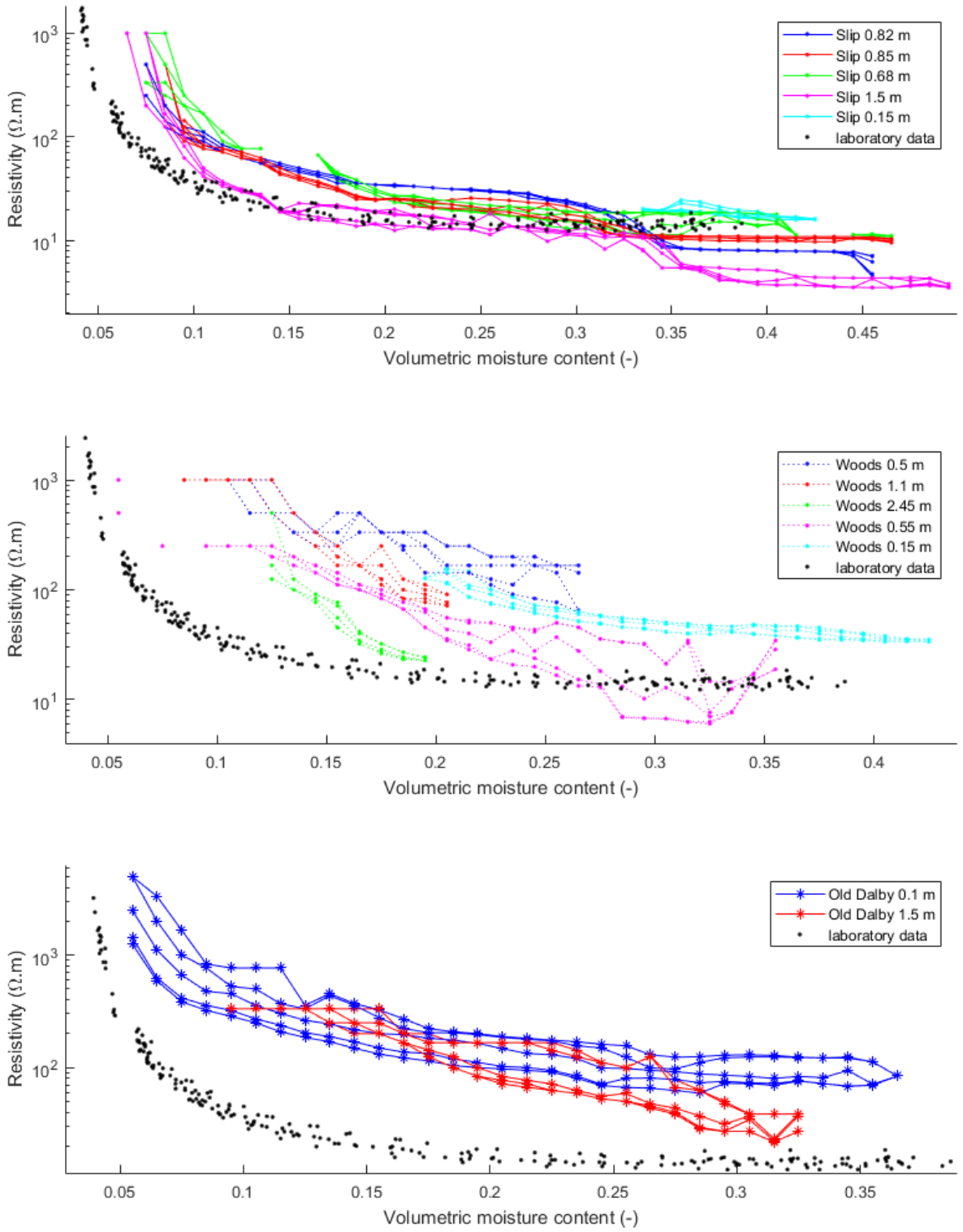


Figure 17: Error on the resistivity measurement. For each sensor the 1st, the 5th, the 50th, the 95th and the 99th percentile of the resistivity measurement is shown.

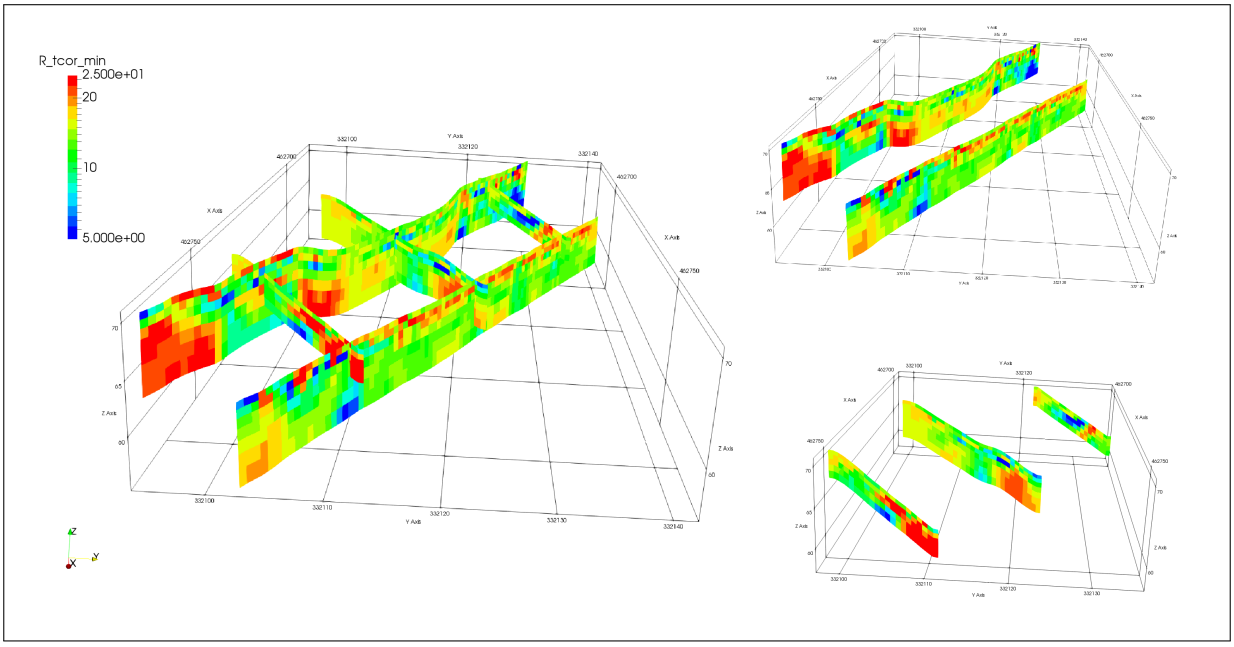


Figure 18: Minimum resistivity observed for each cells (expressed in Ω.m). The minimum observed resistivity is supposed to be close to the saturated resistivity

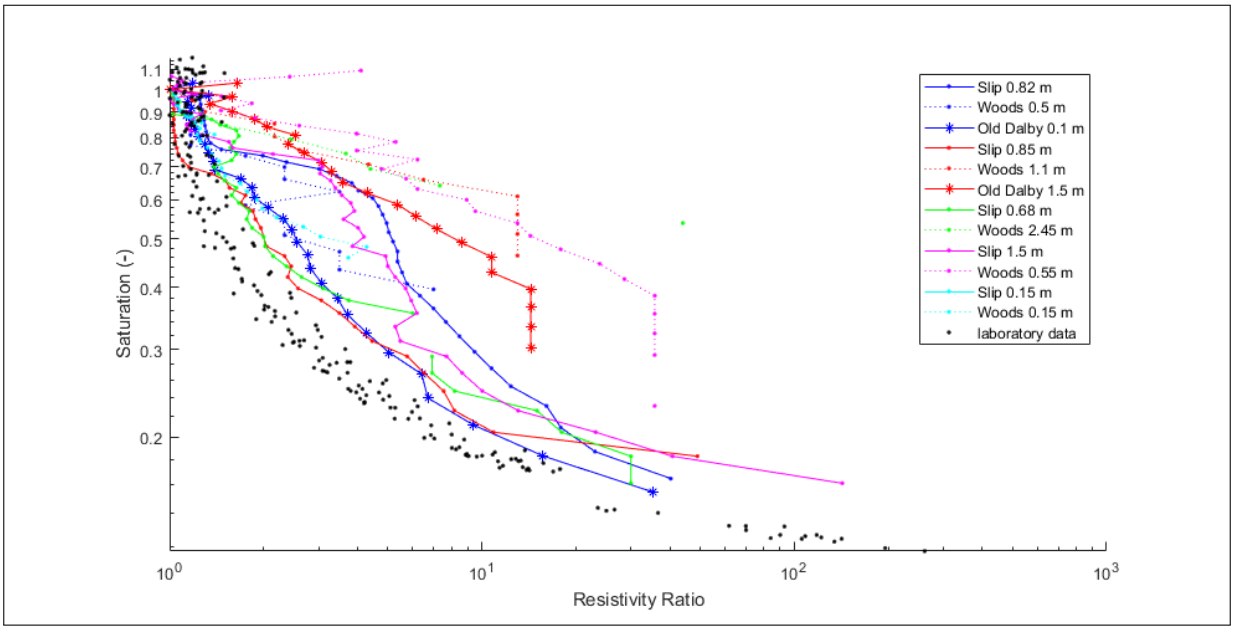


Figure 19: Waxman-Smits on resistivity ratio

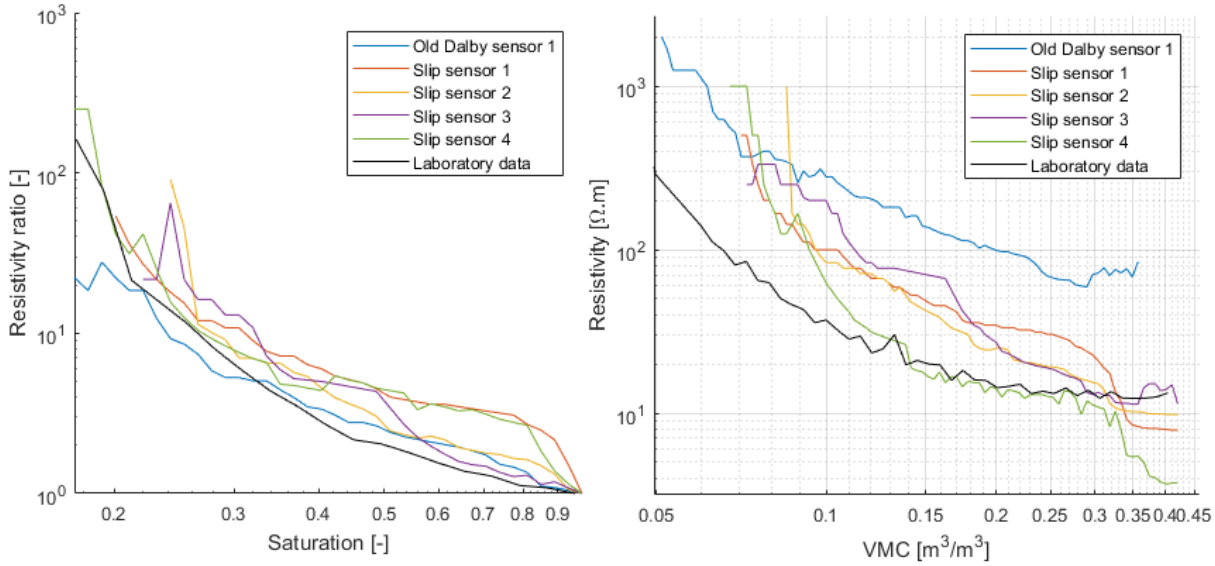


Figure 20: Sensors selected for fitting the Waxman-Smits model. The plotted values corresponds to the median resistivity (resp. resistivity ratio) measured in a given range of VMC (resp. saturation).

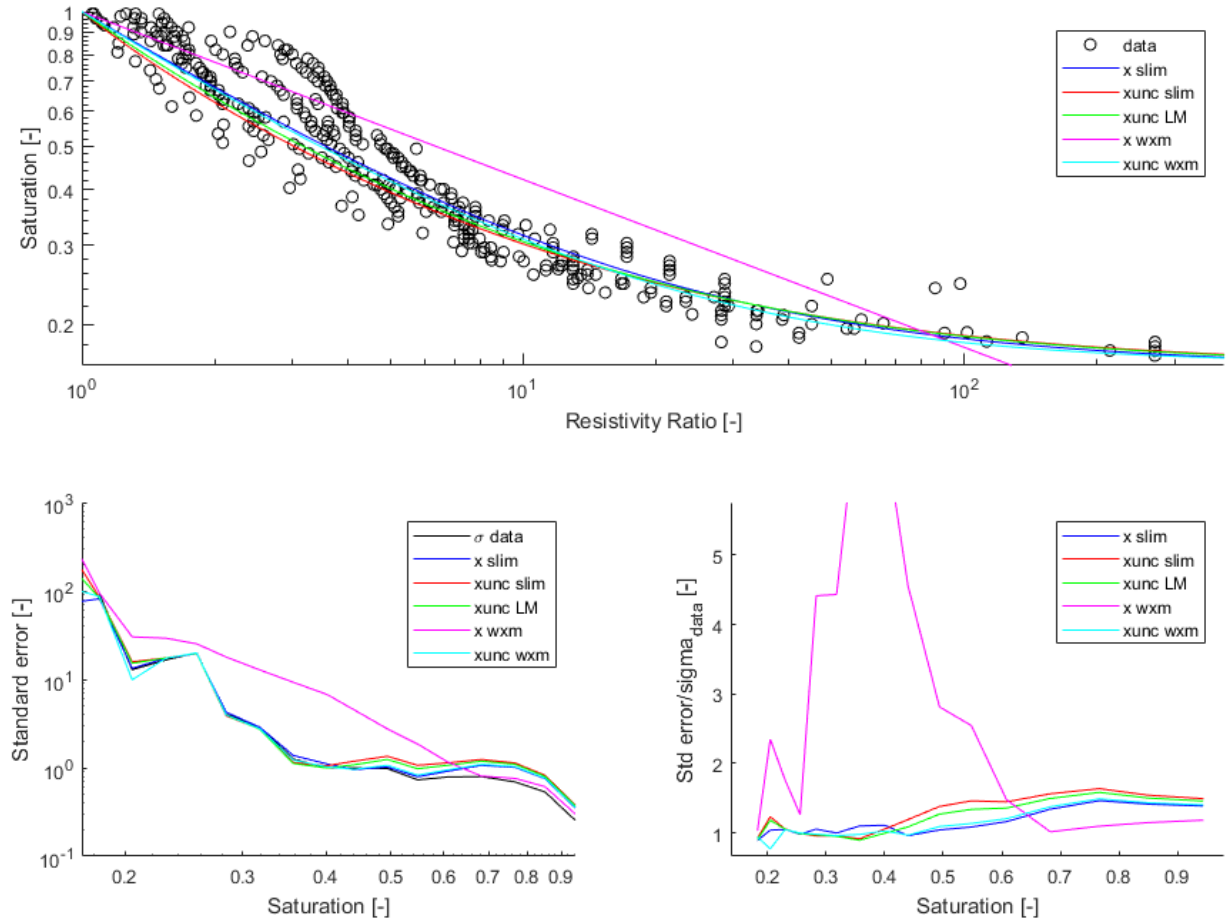


Figure 21: Top figure: Fitting of 5 modified Waxman-Smits model on the selected resistivity dataset. Lower figures: Comparison of the error of the fitted models with the error of the dataset

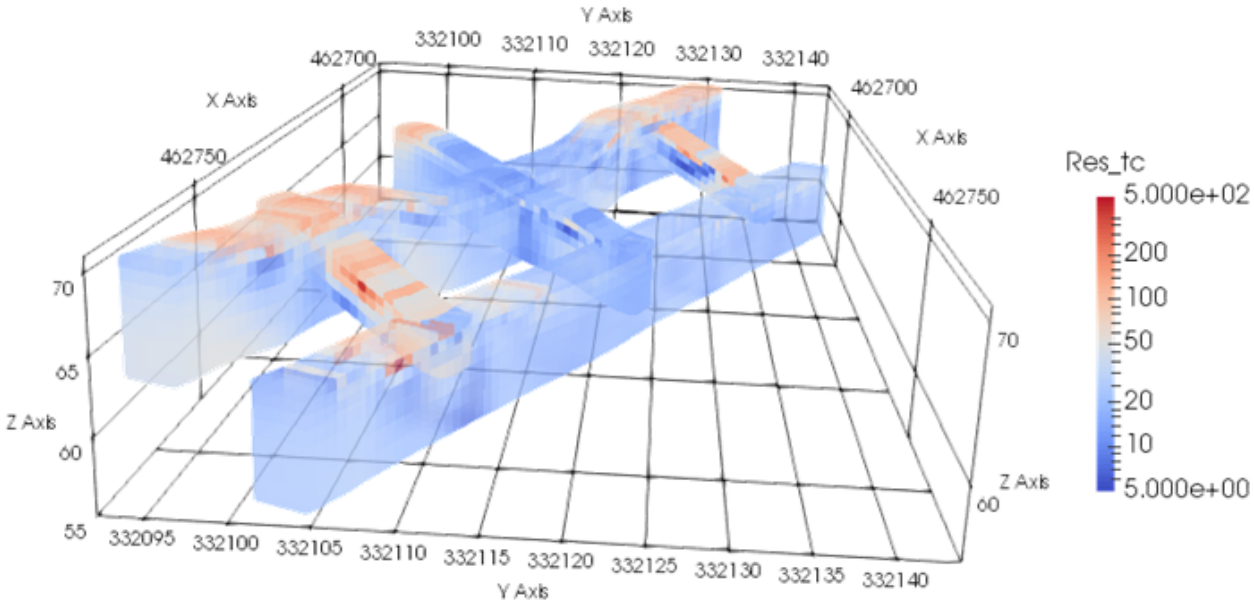


Figure 22: Resistivity (without temperature correction) of the first ERT. Values are expressed in Ω.m

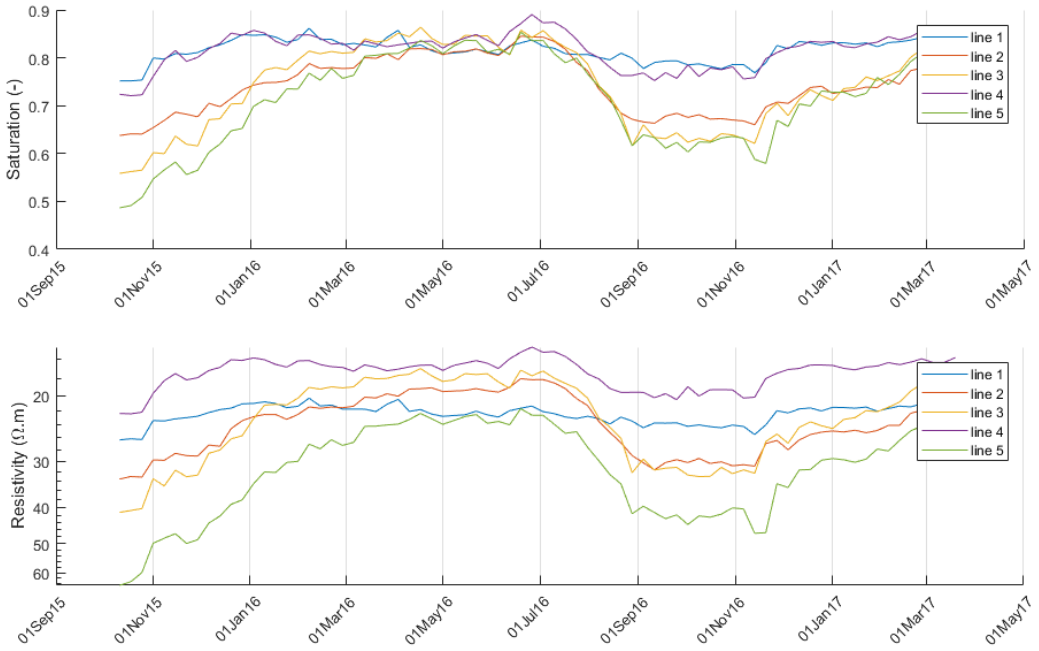


Figure 23: ERT-derived Saturation (subplot 1) and resistivity (subplot 2) mean values calculated for the first three meters of each lines.

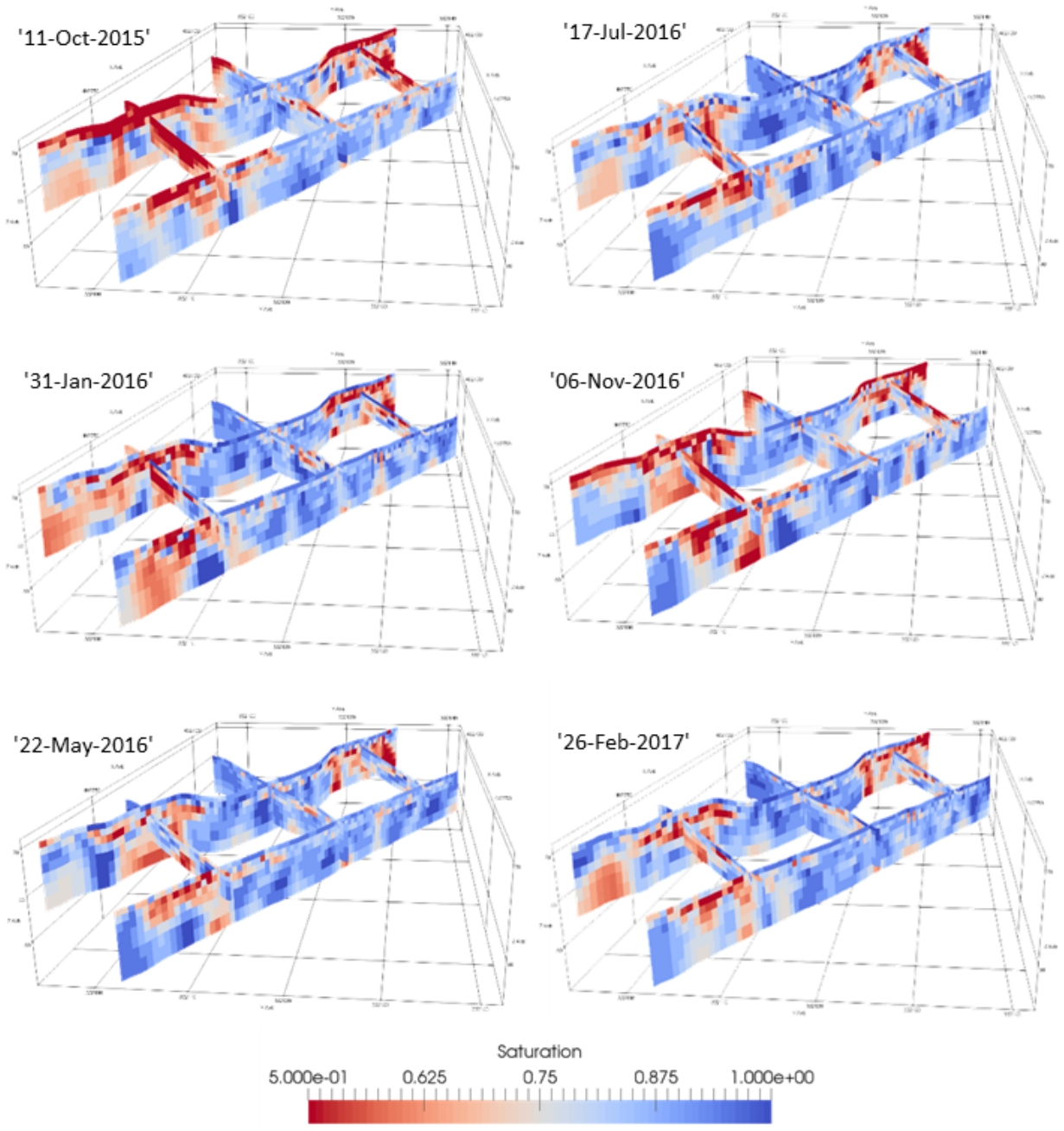


Figure 24: ERT derived saturation imaging of the subsoil

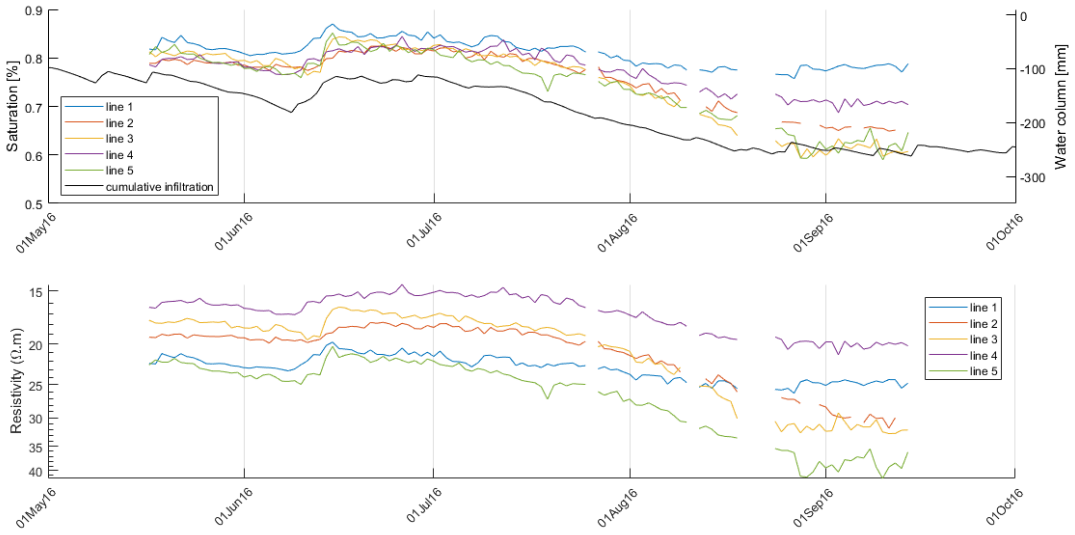


Figure 25: ERT-derived Saturation (subplot 1) and resistivity (subplot 2) mean values calculated for the first three meters of each lines.

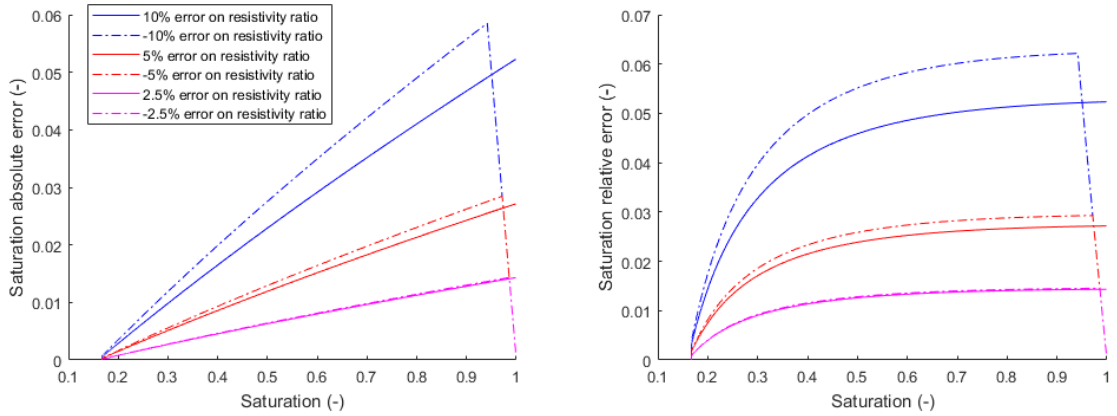


Figure 26: Effect of resistivity ratio error on saturation evaluation

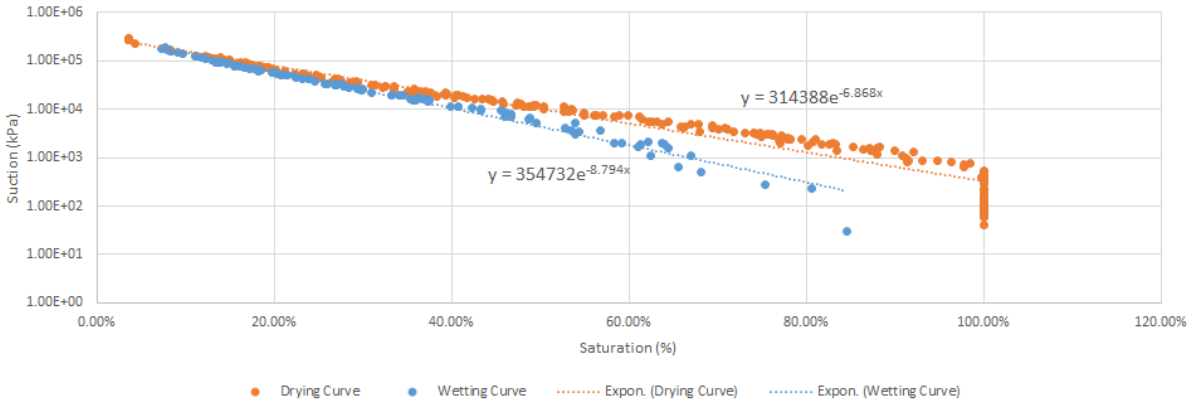


Figure 27: Water retention curve established from laboratory testing of compacted material drilled on site

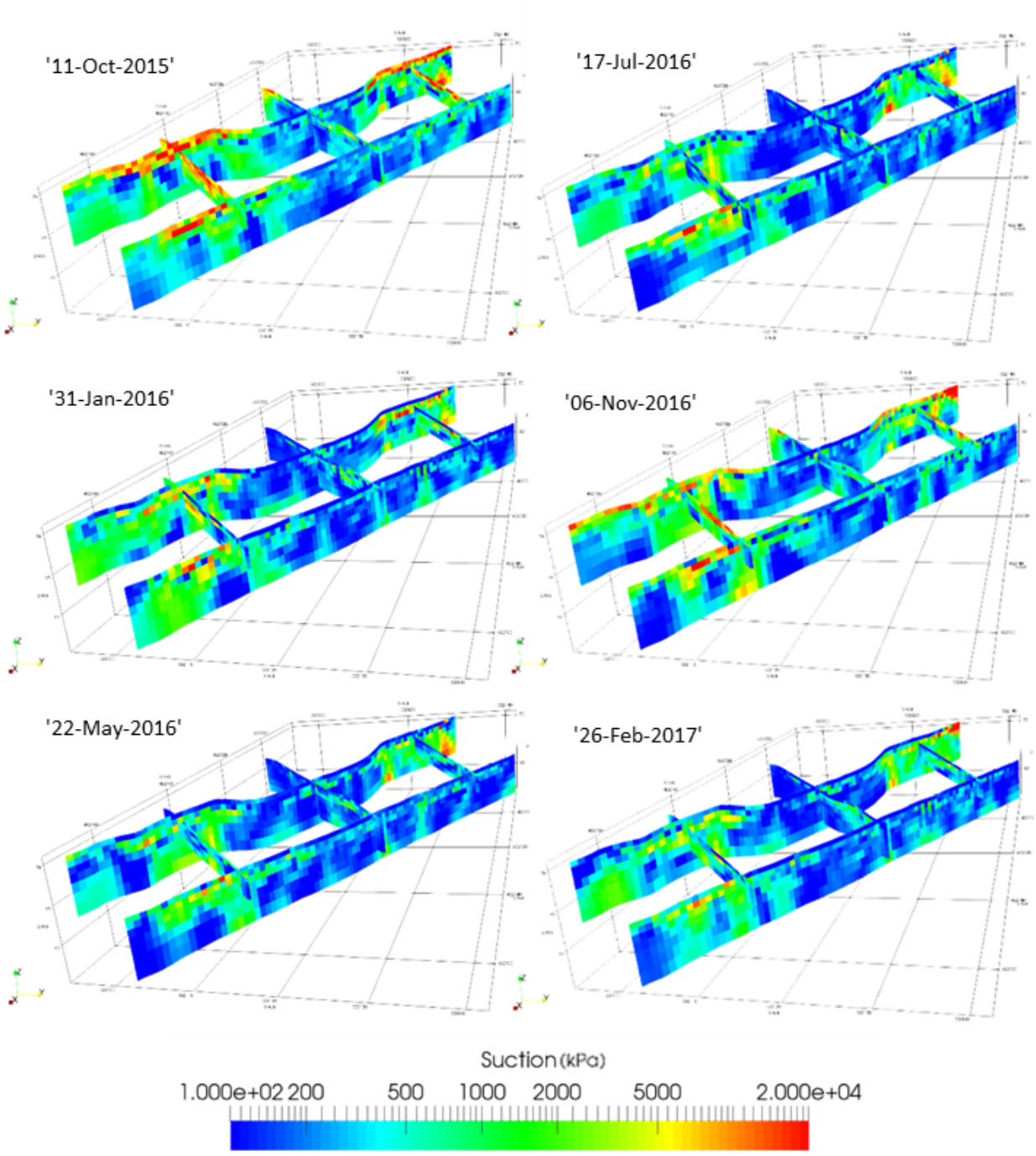


Figure 28: ERT-derived suction imaging of the subsoil